Notes on Kerr cavity beyond bifurcation

Bhargava Thyagarajan

18th August 2021

We begin by considering a Kerr cavity such as the cCPT system as in eqn. (C1) of [1].

$$H = \hbar\omega_0 a^\dagger a + \frac{1}{2}\hbar K a^{\dagger 2} a^2 \tag{1}$$

$$= \hbar(\omega_0 + \frac{K}{2}a^\dagger a)a^\dagger a - \frac{1}{2}\hbar K a^\dagger a \tag{2}$$

$$\approx \hbar(\omega_0 + \frac{K}{2}a^\dagger a)a^\dagger a \tag{3}$$

where ω_o is the bias point dependent resonant frequency, K is the strength of the Kerr term at the bias point, and we neglect the last term in the Hamiltonian because $K < \kappa_{tot}$ and $K \ll \omega_0$ for our cCPT system across all gate and flux biases.

Writing down the quantum Langevin equation for this Hamiltonian, we get

$$\dot{a} = \frac{1}{i\hbar}\big[a, H\big] - \big[a, a^\dagger\big]\big[\frac{\kappa_{tot}}{2}a - \sqrt{\kappa_{ext}}a_{in}(t) - \sqrt{\kappa_{int}}b_{in}(t)\big] \tag{4}$$

$$= -\big[i(\omega_0 + Ka^\dagger a) + \frac{\kappa_{tot}}{2}\big]a + \sqrt{\kappa_{ext}}a_{in}(t) + \sqrt{\kappa_{int}}b_{in}(t) \tag{5}$$

where κ_{ext} is the external damping rate because of the coupling to the probe transmission line with the corresponding input bath operator $a_{in}(t)$, and κ_{int} is the internal damping rate because of the coupling of the resonator to an internal loss channel (typically a thermal bath) with corresponding input operator $b_{in}(t)$. The total damping rate of the cavity is $\kappa_{tot} = \kappa_{ext} + \kappa_{int}$.

The input tone is a pure sine wave at frequency ω_d of the form $a_{in} = \alpha_{in}e^{-i\omega_d t}$. We expect the steady state response of the cavity to be at this drive frequency. We thus make the ansatz $a = \alpha e^{-i\omega_d t}$, $\dot{a} = -i\omega_d^{-i\omega_d t}$ and the average cavity occupation $n = |\alpha|^2 = a^\dagger a$. Plugging this ansatz into (5) and we obtain

$$\big[-i(\Delta - K|\alpha|^2) + \frac{\kappa_{tot}}{2}\big]\alpha = \sqrt{\kappa_{ext}}\alpha_{in}$$

and

$$\big[i(\Delta - K|\alpha|^2) + \frac{\kappa_{tot}}{2}\big]\alpha^* = \sqrt{\kappa_{ext}}\alpha^*_{in} \tag{6}$$

where we have defined the detuning $\Delta = \omega_d - \omega_0$

We can now use eqn.(6) and the input-output relation $a_{out}(t) = a_{in}(t) - \sqrt{\kappa_{ext}}a(t)$ [2], [3] to find the reflection coefficient $S_{11}(\Delta)$ (eqn.C9 in [1]) to be

$$\begin{aligned} S_{11}(\Delta) &= \left(\frac{\alpha_{out}}{\alpha_{in}}\right)^* \\ &= \frac{(\Delta - K|\alpha|^2) - i(\kappa_{int} - \kappa_{ext})/2}{(\Delta - K|\alpha|^2) - i(\kappa_{int} + \kappa_{ext})/2} \end{aligned} \tag{7}$$

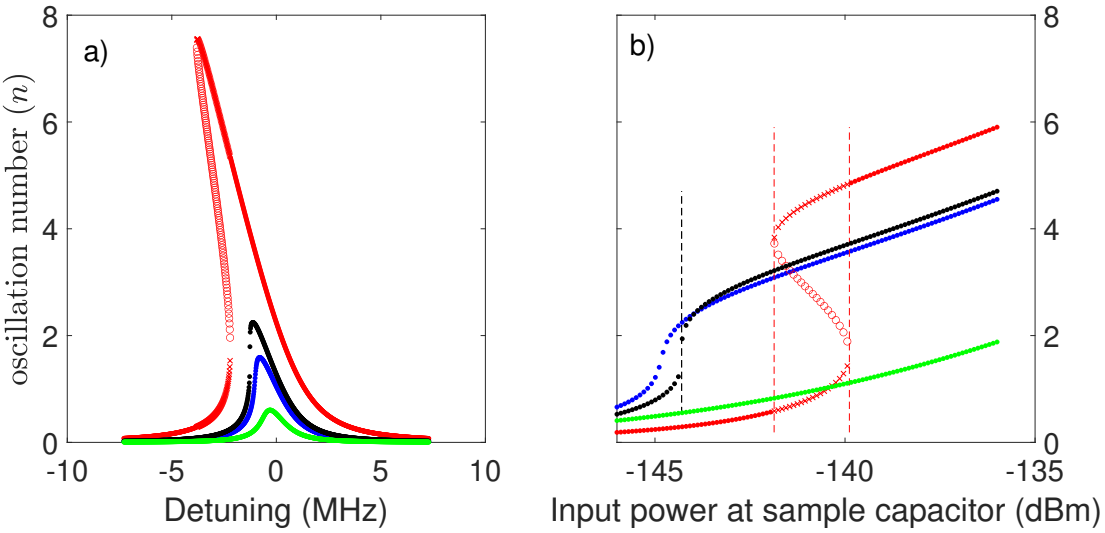

Figure 1: (a) Oscillation amplitude as a function of detuning for different input drive powers. The green markers are for an essentially linear cavity with $P_{in} \ll P_{in_c}$ (see eqn. (13)), blue markers are when driven with a $P_{in} < P_{in_c}$, the black is when $P_{in} = P_{in_c}$ and the red is when $P_{in} > P_{in_c}$. (b) Oscillation amplitude as a function of input power for different detunings. The green markers are for $\Delta > 0$, the blue markers are when $\Delta_c < \Delta < 0$ (see eqn. (12), the black markers are for $\Delta = \Delta_c$ and the red markers are for $\Delta < \Delta_c$. The dots represent monostable solutions, the crosses - bistable solutions, and the unfilled circles represent unstable solutions in both plots. These values are simulated for $K = -0.5$MHz which occurs at $(n_g, \varphi_{ext}) = (0, 0)$. $\kappa_{ext} = 1.2323$MHz, $\kappa_{int} = 0.226$MHz and $\omega_0 = 5.7851$GHz at this bias point.

Multiplying the two equations in (6), we get a cubic in n

$$K^2n^3 - 2K\Delta n^2 + \big(\Delta^2 + \frac{\kappa_{tot}^2}{4}\big)n = \kappa_{ext}\frac{P_{in}}{\hbar\omega_d} \tag{8}$$

where $P_{in} = n_{in}\hbar\omega_d$ and $n_{in} = |\alpha_{in}|^2$.

Solving this cubic for n and plugging those solutions into eqn.(7), we obtain the amplitude and phase response of the cavity to a given drive.

In the presence of the Kerr non-linearity, the system can exhibit different types of oscillation behaviours as the drive power P_{in} and the detuning Δ are varied. At small drive strengths when the effect of the non-linearity is small, we see only a monostable oscillation amplitude as for a linear oscillator. As the drive strength is increased, for a certain range of detunings, we see this stable oscillation state bifurcate into two stable higher and lower oscillation states along with an unstable state that is not experimentally observed. The system has bifurcated into a bistable regime (fig. 1). The onset of bistability is marked by the slope of the n vs Δ curve becoming vertical at some value of detuning (black curve in fig. 1a). i.e, $\frac{dn}{d\Delta} = \infty$ for some Δ.

Differentiating (8) w.r.t n, and setting $\frac{d\Delta}{dn}\big|_{n_c} = 0$, we have

$$3K^2n_c^2 - 4K\Delta n_c - 2Kn_c^2\left.\frac{d\Delta}{dn}\right|_{n_c} + \Delta^2 + \frac{\kappa_{tot}^2}{4} + 2\Delta n_c\left.\frac{d\Delta}{dn}\right|_{n_c} = 0 \tag{9}$$

$$\implies 3K^2n_c^2 - 4K\Delta n_c + \big(\Delta^2 + \frac{\kappa_{tot}^2}{4}\big) = 0 \tag{10}$$

where n_c is the oscillation number at the onset of bifurcation. Solving this quadratic equation (10), we solve for the critical oscillation number obtaining

$$n_c = \frac{2\Delta}{3K}\big(1 \pm \frac{1}{2}\sqrt{1 - \frac{3\kappa_{tot}^2}{4\Delta^2}}\big) \tag{11}$$

This yields real, positive solutions when

$$\Delta < -\frac{\sqrt{3}}{2}\kappa_{tot} \;\forall\; K < 0$$

$$\Delta > \frac{\sqrt{3}}{2}\kappa_{tot} \; \forall \; K > 0 \tag{12}$$

To achieve bifurcation at exactly this critical detuning $\Delta_c = \text{sgn}(K)\frac{\sqrt{3}}{2}\kappa_{tot}$, we see from eqn. (11) that we need a critical cavity occupation number $n_c = \frac{1}{\sqrt{3}}\frac{\kappa_{tot}}{K}$. Using these in (8), we obtain a critical drive power P_{in_c}. When the cavity is driven by a tone at $\omega_{d_c} = \omega_0 + \Delta_c$ with amplitude exactly P_{in_c}, we see the onset of bistability, where

$$P_{in_c} = \frac{\sqrt{3}}{9}\frac{\kappa_{tot}^3}{|K|\kappa_{ext}}\hbar\omega_{d_c} \tag{13}$$

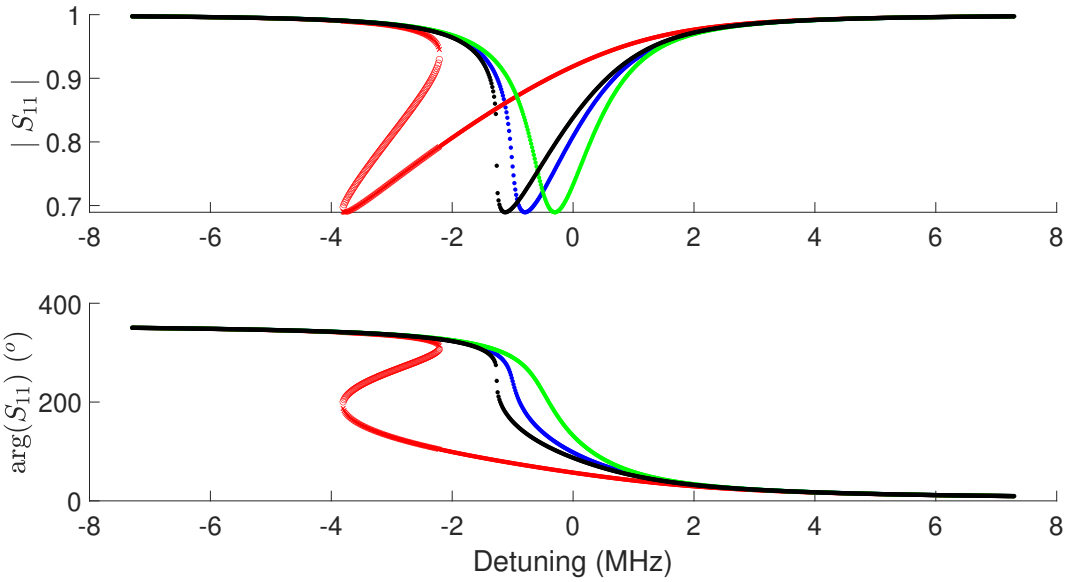

Figure 2: S_{11} as a function of detuning for different input drive powers. The green markers are for an essentially linear cavity with $P_{in} \ll P_{in_c}$ (see eqn. (13)), blue markers are when driven with a $P_{in} < P_{in_c}$, the black is when $P_{in} = P_{in_c}$ and the red is when $P_{in} > P_{in_c}$. The dots represent monostable solutions, the crosses - bistable solutions, and the unfilled circles represent unstable solutions. These values are simulated for $K = -0.5$MHz which occurs at $(n_g, \varphi_{ext}) = (0, 0)$. $\kappa_{ext} = 1.2323$MHz, $\kappa_{int} = 0.226$MHz and $\omega_0 = 5.7851$GHz at this bias point.

Figs.(2) and (3), plotted using eqn.(7), show the variation of the reflection coefficient (S_{11}) with detuning and drive power respectively. We clearly see the jump phenomenon in fig.(2).

As the detuning is ramped from a value well red-detuned from the linear resonance, S_{11} follows the value corresponding to the monostable solution. Even after the lower bifurcation detuning value at which we first expect to see bistability, it stays on the same branch of the S_{11} corresponding to the low amplitude oscillation state until it reaches the value of the detuning where the second bifurcation occurs. As the detuning is increased past this value, S_{11} has to jump abruptly to the monostable value on the other side of this upper bifurcation. When the detuning is ramped in the other direction, the S_{11} stays on the branch corresponding to the high amplitude oscillation state, past the upper bifurcation, until it reaches the detuning value at the lower bifurcation. It must then jump abruptly and proceed along the monostable branch of the S_{11} at lower values. This gives rise to a marked

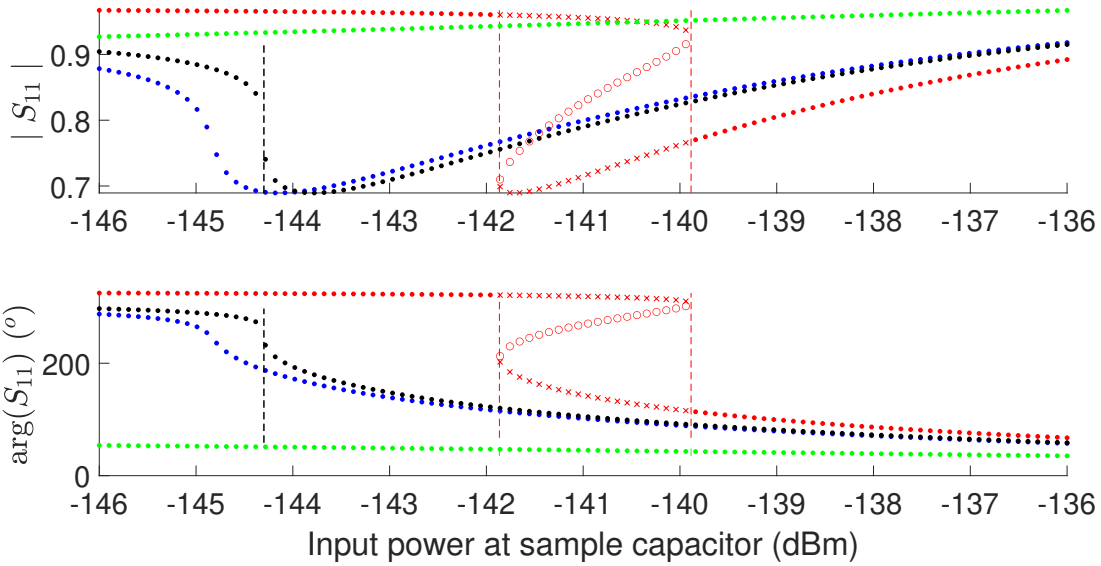

Figure 3: S_{11} as a function of input power for different detunings. The green markers are for a detuning $\Delta > 0$, blue markers are when driven at a detuning $\Delta_c < \Delta < 0$, the black is when $\Delta = \Delta_c$ and the red is when $\Delta < \Delta_c$. The dots represent monostable solutions, the crosses - bistable solutions, and the unfilled circles represent unstable solutions. The dotted lines represent the input powers at the onset of bistability, calculated from eqn. (15). These plots are simulated for $K = -0.5$MHz which occurs at $(n_g, \varphi_{ext}) = (0, 0)$. $\kappa_{ext} = 1.2323$MHz, $\kappa_{int} = 0.226$MHz and $\omega_0 = 5.7851$GHz at this bias point.

hysteresis in the S_{11} curves depending on which way the detuning is ramped as seen in fig. (4). A similar jump phenomenon (fig. 2) and hysteresis is observed as P_{in} is ramped in each direction, as seen in fig. (5).

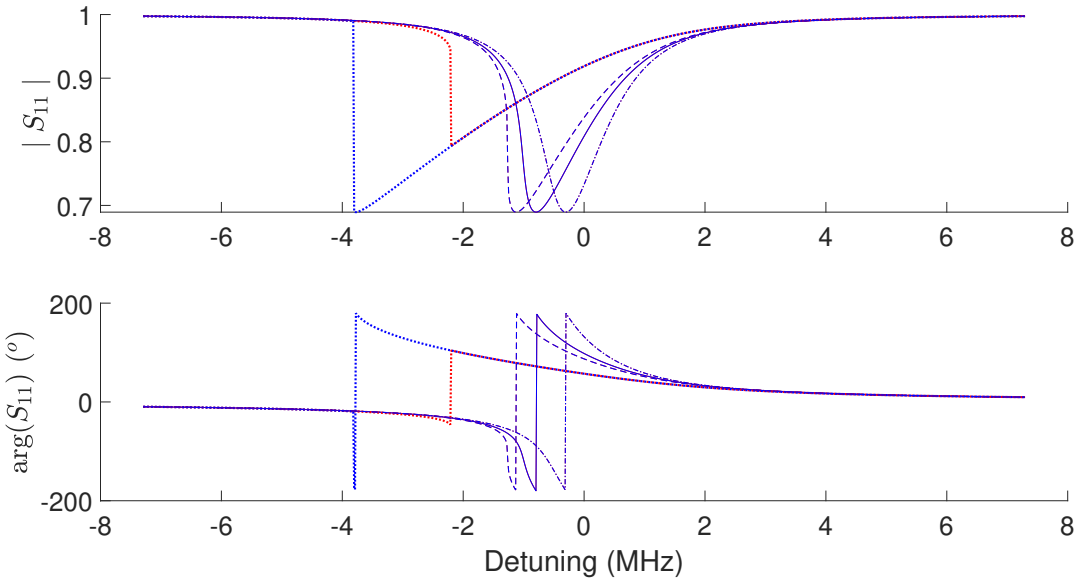

Figure 4: Hysteresis in S_{11} as a function of detuning for different input drive powers. The dash-dotted lines are for an essentially linear cavity with $P_{in} \ll P_{in_c}$ (see eqn. (13)), solid lines are when driven with a $P_{in} < P_{in_c}$, the dashed is when $P_{in} = P_{in_c}$ and the dotted is when $P_{in} > P_{in_c}$. Red traces represent a ramp that sweeps towards increasing frequency, and the blues ramp toward decreasing frequency. The blue and red overlap for $P_{in} \leq P_{in_c}$. These values are simulated for $K = -0.5$MHz which occurs at $(n_g, \varphi_{ext}) = (0, 0)$. $\kappa_{ext} = 1.2323$MHz, $\kappa_{int} = 0.226$MHz and $\omega_0 = 5.7851$GHz at this bias point.

This sudden jump at the input power bifurcation forms the basis for the operation of the Josephson Bifurcation Amplifier (JBA) [4]. The sensitivity of an amplifier to a change in the drive power is the slope of the phase-input power curve at any point. When there is only monostable behaviour, we see that the phase is a linear function of the input power for small variations about any input power bias point. However, by carefully biasing the JBA right at a drive power bifurcation edge, a very small change in the drive power leads to a large shift in the phase response of the amplifier. Monitoring the output phase, we thus have

a sensitive measure of very small variations in the input power/current.

In order to find the extent of the bistability region as a function of the input drive strength (for a given detuning Δ), we find the bifurcation points $P_{in_{b_1}}$ and $P_{in_{b_2}}$ where $\frac{dn}{dP_{in}}\Big|_{P_{in_{b_1}},P_{in_{b_2}}} = \infty$. Between these points, we expect to see bistability. We thus differentiate eqn. (8) with respect to n and set $\frac{dP_{in}}{dn}\Big|_{P_{in_{b_1}},P_{in_{b_2}}} = 0$ yielding

$$n_{P_{in_{b_1}},P_{in_{b_2}}} = \frac{2}{3}\frac{\Delta}{K}\left[1 \pm \frac{1}{2}\sqrt{(1 - \frac{3\kappa_{tot}^2}{4\Delta^2})}\right] \tag{14}$$

Using these solutions in eqn. (8), we find the bifurcation points to be

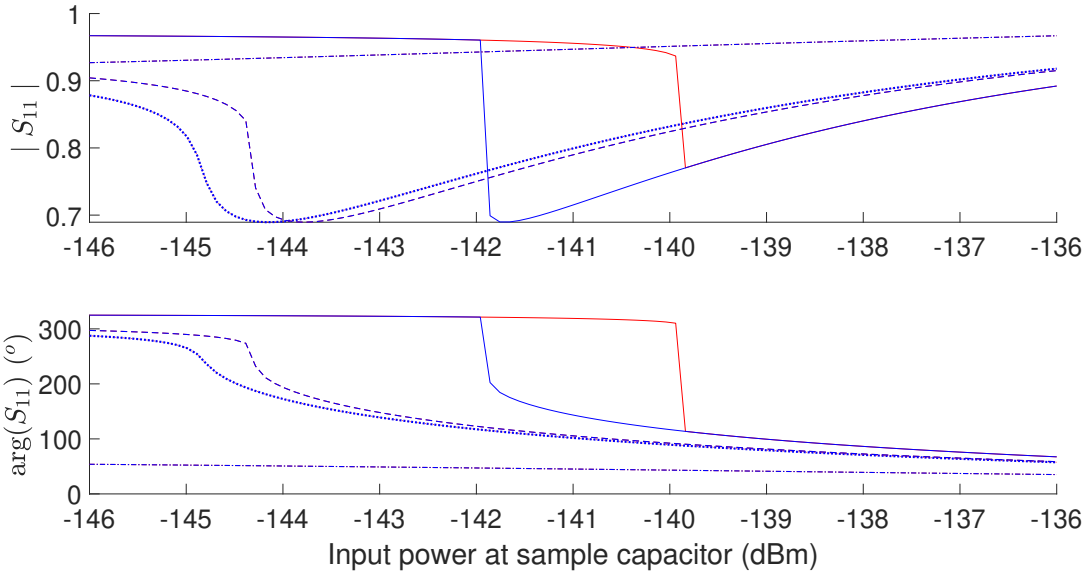

Figure 5: Hysteresis in S_{11} as a function of drive power for different detunings. The dash-dotted lines are for a detuning $\Delta > 0$, the dotted are for $0 < \Delta < \Delta_c$, the dashed are for $\Delta = \Delta_c$, and the solid lines are for $\Delta < \Delta_c$. The red traces represent an increase in drive power with time, and the blue traces represent a decrease in drive power with time. The red and blue curves overlap for $\Delta \geq \Delta_c$. These values are simulated for $K = -0.5$MHz which occurs at $(n_g, \varphi_{ext}) = (0, 0)$. $\kappa_{ext} = 1.2323$MHz, $\kappa_{int} = 0.226$MHz and $\omega_0 = 5.7851$GHz at this bias point.

$$P_{in_{b_1}}, P_{in_{b_2}} = \frac{2}{27}\frac{\Delta^3}{K}\left[\left(1+\frac{9\kappa_{tot}^2}{4\Delta^2}\right) \mp \left(1-\frac{3\kappa_{tot}^2}{4\Delta^2}\right)^{3/2}\right]\frac{\hbar\omega_d}{\kappa_{ext}} \tag{15}$$

which corresponds to eqn. (2.13) in [5].

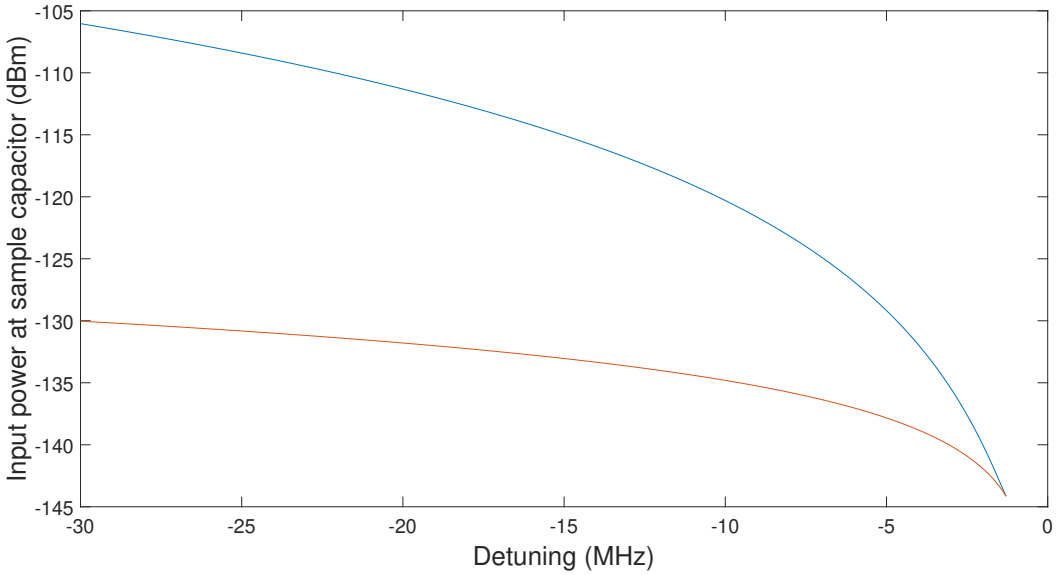

Figure 6: Variation of input power at the plane of the sample required for the onset of bifurcation vs detuning. The red (blue) corresponds to the lower (upper) bifurcation point for $K = -0.5$MHz which occurs at $(n_g, \varphi_{ext}) = (0, 0)$. $\kappa_{ext} = 1.2323$MHz, $\kappa_{int} = 0.226$MHz and $\omega_0 = 5.7851$GHz at this bias point.

Plotting the lower and upper bifurcation powers as a function of detuning, we see that for larger detunings, the bistability region begins at a larger input power, and is also broader. Since we typically see larger phase shifts at the lower bifurcation point in our experiments, we drive the cCPT at a large enough detuning that the standard deviation of the measured phase at the larger lower bifurcation point is small compared to the difference in the phases of the two bistable states. This standard deviation is a function of the SNR of the output signal where the noise is fixed by the noise temperature and bandwidth of the measurement setup. This means the SNR increases with increasing signal strength, and we want to work at relatively (w.r.t single photon levels) large input powers, corresponding to larger detunings, see fig.(6).

We envision a charge sensing scheme similar to the power/current readout of the JBA. At a certain drive power, by biasing the cCPT at the edge of a bifurcation in detuning, the output phase should be very sensitive to small changes in the detuning and hence the resonant frequency of the cCPT. This resonant frequency of the cCPT is itself a pretty sensitive function of the gate charge (n_g) of the cCPT [1]. The sensitivity will be determined by biasing to the bifurcation point and then putting in a increasingly larger gate steps, to see what the smallest detectable value of the step is. This would be the metric for the charge sensitivity. Confounding factors for such a measurement would be : i) the spontaneous thermal hopping between the metastable high and low amplitude states of the cCPT when in a bistable regime as modelled in [**?**]. This can be circumvented by instead measuring the 'S-curves' which are a plot of the probability of being in the low amplitude state as a function of the detuning. The metric for charge sensitivity then becomes the smallest gate charge that causes a perceptible shift in the S-curves. ii) resonant frequency fluctuations as reported in [1]. These could cause the resonant frequency to spontaneously shift due to fluctuations in the charge or flux environment on the cCPT chip, or due to quantum fluctuations in photon number. This can be imagined as causing each S-curve to have a finite, non-zero width which is a function of σ_{omega_0} (see eqn.(24) in [1]), and the minimum perceptible change between two S-curves has to be larger than the combined widths of the two.

References

[1] B. Brock, J. Li, S. Kanhirathingal, B. Thyagarajan, W. F. Braasch, M. Blencowe, A. Rimberg, Nonlinear charge- and flux-tunable cavity derived from an embedded cooper-pair transistor, Phys. Rev. Applied 15 (2021) 044009. doi:10.1103/PhysRevApplied.15.044009.
URL https://link.aps.org/doi/10.1103/PhysRevApplied.15.044009

[2] C. W. Gardiner, M. J. Collett, Input and output in damped quantum systems: Quantum stochastic differential equations and the master equation, Phys. Rev. A 31 (1985) 3761–3774. doi:10.1103/PhysRevA.31.3761.
URL https://link.aps.org/doi/10.1103/PhysRevA.31.3761

[3] C. Gardiner, P. Zoller, Quantum Noise: A Handbook of Markovian and Non-Markovian Quantum Stochastic Methods with Applications to Quantum Optics, Springer Series in Synergetics, Springer, 2004.
URL https://books.google.com/books?id=a_xsT8oGhdgC

[4] R. Vijay, M. H. Devoret, I. Siddiqi, Invited review article: The josephson bifurcation amplifier, Review of Scientific Instruments 80 (11) (2009) 111101. arXiv:https://doi.org/10.1063/1.3224703, doi:10.1063/1.3224703.
URL https://doi.org/10.1063/1.3224703

[5] R. Vijayaraghavan, Josephson bifurcation amplifier [electronic resource] : Amplifying quantum signals using a dynamical bifurcation., Ph.D. thesis, available at https://qulab.eng.yale.edu/category/theses/ (2008).